*transplantology*

MDPI

*Review*

# Multimodality Imaging to Detect Rejection, and Cardiac Allograft Vasculopathy in Pediatric Heart Transplant Recipients—An Illustrative Review

**Bibhuti B. Das [1,*], Shriprasad Deshpande [2] and Tarique Hussain [3]**

[1] Pediatric Cardiology, Children's of Mississippi, University of Mississippi Medical Center, Jackson, MS 39216, USA
[2] Pediatric Cardiology, Children's National, The George Washington University, Washington, DC 20010, USA; sdeshpan@childrensnational.org
[3] Pediatric Cardiology, Children's Health, UTSW Medical Center, Dallas, TX 75235, USA; mohammad.hussain@utsouthwestern.edu
* Correspondence: bdas99@hotmail.com; Tel.: +601-984-5250; Fax: 601-984-5283

**Abstract:** The three most common modalities of graft surveillance in pediatric heart transplant (HT) recipients include echocardiography, coronary angiography, and endomyocardial biopsy (EMB). The survival outcomes after HT in children have improved considerably in recent years. However, allograft rejection and cardiac allograft vasculopathy remain the leading cause of death or re-transplantation. The routine surveillance by EMB and coronary angiography are invasive and risky. Newer noninvasive echocardiographic techniques, including tissue Doppler imaging (TDI), 2-D speckle tracking echocardiography, CT coronary angiography (CTCA), cardiovascular magnetic resonance (CMR), single-photon emission computed tomography (SPECT), and positron emission tomography (PET) and invasive techniques such as intravascular ultrasound (IVUS), functional flow reserve (CFR) of coronary arteries, optical coherence tomography (OCT), have emerged as powerful tools which may help early recognition of sub-clinical rejection, response to treatment, early detection, and progression of CAV. The multimodality imaging approach, including noninvasive and invasive tests, is the future for the transplanted heart to detect dysfunction, rejections, and early CAV. This review illustrates noninvasive and invasive imaging techniques currently used or could be considered for clinical use in detecting heart transplant rejection, dysfunction, and CAV in children.

**Keywords:** multimodality imaging; heart transplantation; children; adolescent; cardiac allograft rejection; cardiac allograft vasculopathy



**Citation:** Das, B.B.; Deshpande, S.; Hussain, T. Multimodality Imaging to Detect Rejection, and Cardiac Allograft Vasculopathy in Pediatric Heart Transplant Recipients—An Illustrative Review. *Transplantology* **2022**, *3*, 241–256. https://doi.org/10.3390/transplantology3030025

Academic Editor: Taisto Sarkola

Received: 1 June 2022
Accepted: 5 July 2022
Published: 19 July 2022



## 1. Introduction

Heart transplantation (HT) remains an effective but imperfect therapeutic option for many children with end-stage heart failure. While there has been a significant improvement in pediatric HT recipients' outcomes in recent years, graft failure remains the primary source of morbidity and mortality [1]. Most common causes of cardiac allograft failure in children include acute rejections and cardiac allograft vasculopathy (CAV) [2]. The International Society for Heart and Lung Transplantation (ISHLT) recommends echocardiography as the primary monitoring modality of graft function, followed by coronary angiography and endomyocardial biopsy (EMB) [3]. Per the 2010 ISHLT guidelines, the standard of care in children and adults is to perform periodic EMB during the first 6 to 12 months to monitor for acute rejection (Recommendation Class IIa, Level of evidence C). Selective coronary angiography is the investigation of choice for diagnosing CAV in pediatric HT recipients. It should be performed yearly or biannually (Recommendation Class I, Level of evidence C). At coronary angiography, intravascular ultrasound (IVUS) can be safely carried out in pediatric HT recipients to assess the early stages of CAV (Recommendation Class IIa,

Level of evidence C). Functional coronary flow reserve (CFR) in conjunction with coronary angiography may be helpful in the detection of small-vessel coronary disease, which is an early manifestation of CAV (Recommendation class IIa, Level of Evidence C). The use of EMB later than five years after HT is optional (Recommendation Class IIb, Level of evidence C). The routine clinical use of cardiac magnetic resonance (CMR) imaging for acute allograft rejection monitoring is not recommended (Recommendation Class III, Level of evidence C).

Noninvasive imaging techniques such as tissue Doppler imaging (TDI), speckle tracking echocardiography (STE), stress echocardiography, CT coronary angiography (CTCA), Cardiac MRI (CMR), single-photon emission computed tomography (SPECT), and positron emission tomography (PET) offer new insights into acute rejection, graft dysfunction, and CAV. Furthermore, intracoronary imaging methods such as IVUS and optical coherence tomography (OCT) are emerging tools to detect early CAV. We conducted a comprehensive search to determine if the newer imaging techniques for the transplanted heart have advantages over the conventional methods outlined in updated ISHLT guidelines. We searched the literature on "PubMed", "Scopus", and "Web of Science Core Collection" using keywords of "Pediatric", "Children", Infants", "Adolescents", "Heart transplantation", "Acute allograft rejection", "Cardiac allograft vasculopathy", "Echocardiography", "tissue Doppler imaging", "Speckle tracking echocardiography", " CT coronary angiography", "Intravascular ultrasound", "Fractional flow reserve", "Cardiac magnetic resonance imaging", "Computerized tomography angiography", "Optical Coherence Tomography", "Single-Photon Emission Computed Tomography", and "Positron Emission Tomography" Through 30 April 2022. This paper illustrates a comprehensive review of the different noninvasive and invasive imaging techniques currently used or could be considered for clinical use in detecting HT rejections, graft dysfunction, and CAV.

## 2. Echocardiography

The EMB is the gold standard for the diagnosis of rejection. However, catheterization is an invasive procedure associated with complications inherent in invasive procedures [4]. Echocardiography is the primary testing modality for diagnosing cardiac allograft function [5]. Echocardiography is used in many ways, and the protocols vary from center to enter. Significant variation exists across centers in diagnosing rejection in pediatric HT recipients [6]. In addition, variable echocardiographic strategies may not be independently associated with freedom from rejection, rejection with hemodynamic compromise, or overall graft survival [7].

In the first few days after HT, there is usually an increase in the left ventricular (LV) thickness due to edema, increased perfusion, and inflammatory cell infiltration (Figure 1). Left ventricular mass and wall thicknesses generally normalize within three months, and LV diastolic dysfunction normalizes in 3 to 6 months after HT. Therefore, the presence of LV hypertrophy immediately after HT is considered a normal remodeling process. In addition, Z-scores for LV wall thickness and indexed LV mass are helpful in describing characteristic findings of LV hypertrophy when the heart is from an oversized donor.

Typically, the left ventricular ejection fraction (LVEF) and regional wall motion (except ventricular septal dyskinesia) are preserved in most pediatric HT patients unless multiple rejections or CAV develops. In contrast to evaluating the systolic function, diastolic function assessment is challenging. The diastolic dysfunction or restrictive physiology is expected in the immediate post-transplant period and has no predictive value. However, the persistence of diastolic dysfunction 6-months after transplant has a negative prognostic impact and is often related to inflammation, fibrosis, chronic rejection, and CAV [8]. Noninvasively determined coronary flow reserve (CFR) by echocardiography is an accurate tool for detecting diastolic function associated with CAV in HT recipients [9]. Few studies have evaluated left atrial function and contractile reserve to evaluate the atrial function as a surrogate marker of diastolic function [10]. The newer noninvasive echocardiographic imaging such as TDI, strain, and strain rate analysis by speckle tracking echocardiography

(STE) helps detect myocardial dysfunction. Currently, there is a shift in the paradigm of rejection surveillance from EMB to noninvasive imaging in pediatric HT recipients. A joint European Association of Cardiovascular imaging/Cardiovascular Imaging Department of the Brazilian Society of Cardiology writing group committee has prepared recommendations to provide a practical guide to providers involved in the follow-up of adult HT patients and a framework for standardized and efficient use of cardiovascular imaging [11]. However, there is no comprehensive data for newer echocardiographic imaging modalities in pediatric HT recipients except for small observational studies discussed below.

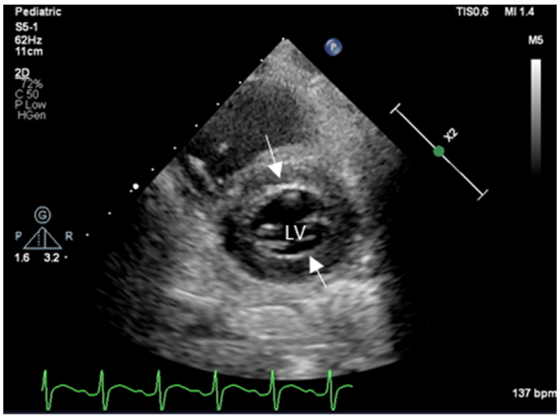


**Figure 1.** Two-Dimensional echocardiography shows a short axis of LV with increased wall thickness due to edema and inflammation immediately after heart transplantation; arrows point to thickened interventricular sept, and LV posterior wall thickness increased (z score + 2).

## 3. Myocardial Deformation Imaging

Over the last decade, TDI and STE have been introduced in clinical echocardiography to quantify myocardial function at the regional level. Notably, LV wall motion and strain analysis improve after a few weeks of HT; therefore, myocardial deformation imaging is not very useful immediately after HT. Myocardial deformation imaging by TDI and STE is independent of cardiac motion and is increasingly being used in adults for serial monitoring of the transplanted heart.

### *3.1. Tissue Doppler Imaging*

TDI-based myocardial deformation imaging can evaluate LV stiffness and diastolic dysfunction [8,12–14]. Both LV myocardial stiffness and diastolic dysfunction in HT recipients are likely due to low-grade subclinical rejection or coronary microvascular diseases. TDI can determine the LV diastolic function by evaluating the longitudinal movement at the mitral, tricuspid, and septal annulus levels, calculating early and late diastolic velocities (E and e', respectively), and comparing these with reference values for children [15]. Mitral and tricuspid valve e' < 5.0 m/s had 93% negative predictive value for rejection [16]. Another study showed that TDI at medial mitral annulus E/e' > 12 is associated with elevated left ventricular end-diastolic pressure (LVEDP) and high-grade cellular rejection, and a lateral tricuspid annulus E/e' > 10 is associated with elevated mean right atrial pressure [17]. However, the role of TDI is controversial in pediatric HT recipients and has resulted in mixed results, as one study demonstrated no correlation with LVEDP [18]. Yet another study showed that EMB-proven rejection is associated with a significant decline in biventricular TDI velocities from baseline [19]. By using well-defined TDI criteria to predict non-rejection, a substantial proportion of planned biopsies can be deferred or avoided in pediatric HT recipients. In addition, many recent studies suggested that TDI parameters help discriminate rejection from non-rejection and can be used as noninvasive surveillance alternatives to EMB [16,20,21]. An example of abnormal LV myocardial velocities in pediatric HT recipients with confirmed rejection by EMB (Grade 2R acute cellular rejection) and

normal TDI in another HT of the same age patient are shown in Figure 2A–D, respectively. The disadvantages of TDI in children include variable results with different vendors and the absence of normal reference values established for pediatric HT recipients. The advantage of TDI includes higher temporal resolution and less image dependence.

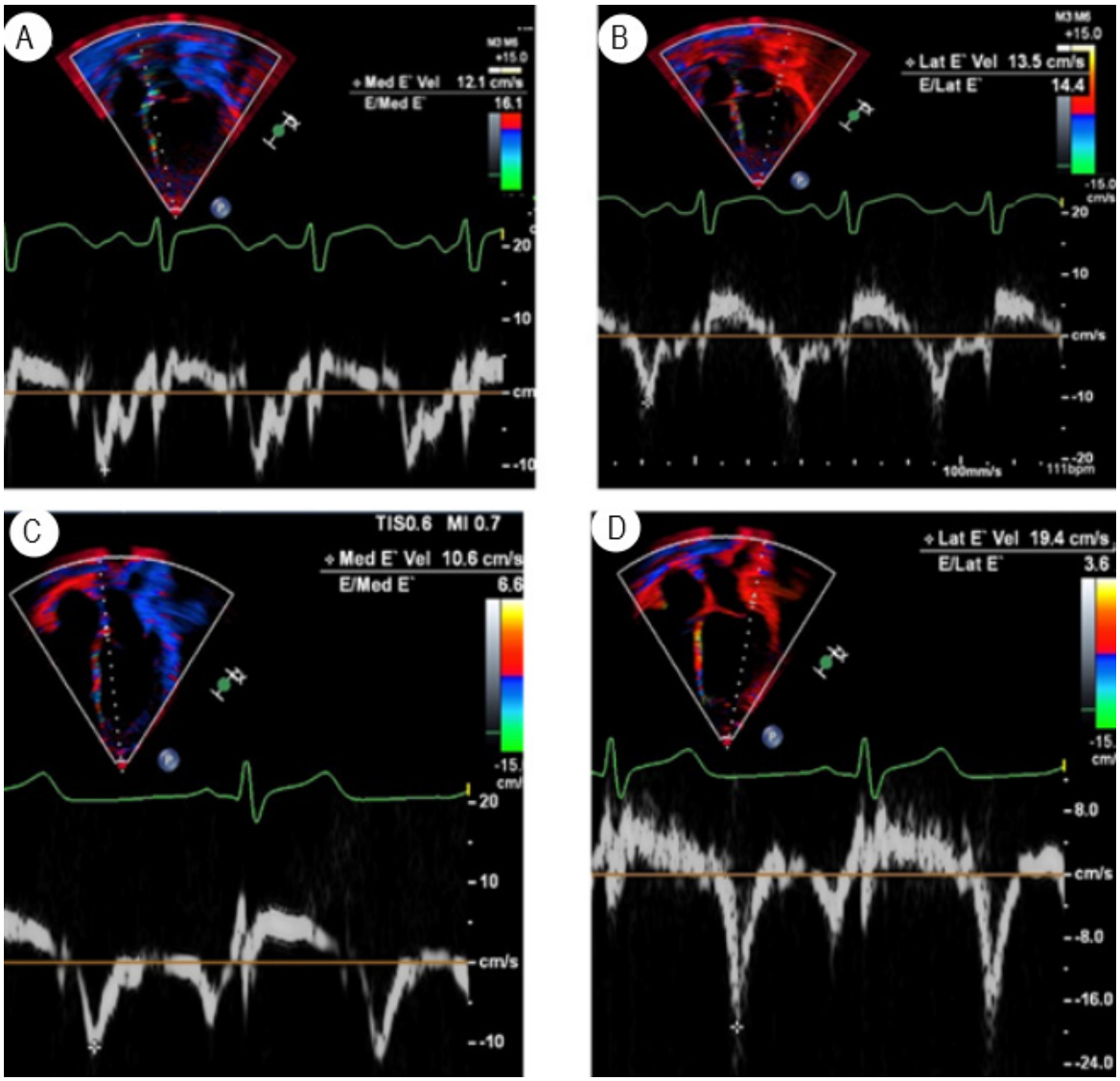


**Figure 2.** (**A**) TDI of the medial mitral annulus and (**B**) lateral annulus of the mitral valve in a six-year-old female three months post-transplant, showing diastolic dysfunction. E/e' at medial mitral annulus 16.1 and at lateral annulus 14.4. (**C**,**D**) show the normal TDI at the medial and lateral annulus of the mitral valve in another 6-yr-old HT recipient who is doing well.

### *3.2. Speckle Tracking Echocardiography*

Left ventricle ejection fraction (LVEF) and fractional shortening (LVFS) are standard methods of quantifying LV systolic function. However, after HT, altered geometry of ventricles, resting tachycardia, and abnormal septal motion occur, making standard echocardiography less sensitive to detect early dysfunction, rejection, or CAV. Strain and strain rate analysis allows quantifying myocardial function at the regional level. STE is a more precise method for quantifying LV function in pediatrics, with lower variability than LVEF and LVFS [22]. Calculating strain and strain rate by 2-D STE in children has also been shown to correlate with LVEDP [23–25]. Global longitudinal strain (GLS) is the most common strain analysis used in pediatric HT recipients. Several small studies found that noninvasive

GLS is sensitive and specific in identifying acute clinical rejection in pediatric HT recipients [6,26–29]. Speckle tracking strain and strain rate imaging were also helpful in defining low-grade rejection in children after HT [30]. GLS by speckle tracking echocardiography imaging correlates better with invasive measurement of LVEDP than traditional echocardiographic parameters [31,32]. The STE strain imaging is also valuable for detecting the early development of CAV in children after HT [33]. An example of 2-D speckle tracking imagine differentiating no-rejection versus chronic rejection in a pediatric HT recipient is shown in Figure 3A–C. The advantage of STE is higher spatial resolution and is angle independent. The disadvantages are similar to TDI, no normal values are established in pediatric HT recipients, and there is a learning curve for this modality among technicians and physicians.

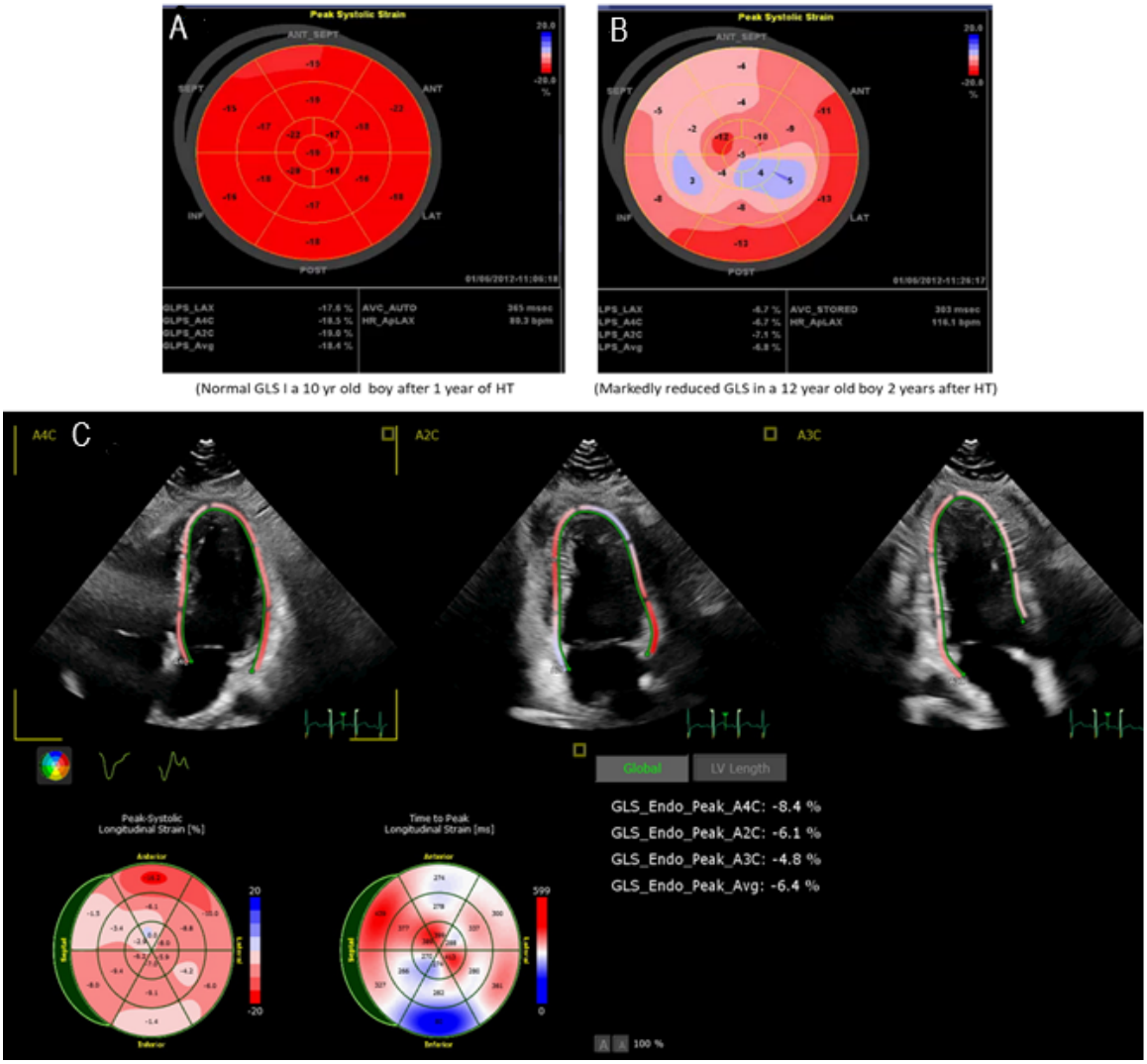


**Figure 3.** (**A**) Normal global longitudinal strain, (**B**) Markedly decreased global longitudinal strain; and (**C**): Average of global longitudinal strain, markedly decreased in a 15-year-old boy after 2 years of HT.

### *3.3. Stress Echocardiography*

Pediatric HT recipients > 6 years of age can exercise safely; however, their exercise tolerance is reduced, and LV contractility is reduced compared to healthy controls [34]. Stress echocardiography can also be carried out with inotropes such as dobutamine induction of stress. The goal of stress is to achieve the target heart rate. Echocardiographic abnormalities

such as regional wall motion abnormalities during dobutamine stress echocardiography correlated with CAV in pediatric HT recipients [35–37]. However, there are disparate results in dobutamine stress echocardiography as the sensitivity rates vary between 35% and 71%, specificity between 80% and 94%, the positive predictive value between 45% and 91%, and negative predictive value between 81% and 92% [38,39]. Conversely, TDI for LV function during the supine bicycle exercise test was preserved [40]. Assessment of LV GLS during exercise stress test is also feasible and strongly associated with the presence and the degree of CAV [41]. The disadvantages of stress echocardiography are operator dependency, low quality of images, need to achieve a target heart rate, risk of arrhythmia, low sensitivity, and may not be positive in early CAV.

## 4. Computed Tomography Coronary Angiogram

CT coronary angiography (CTCA) has higher sensitivity and specificity for diagnosing CAV compared to stress echocardiography. It has been used in adults for routine detection of CVA with good image quality and low radiation dose [42]. With photon-counting CT, we are entering a new era that decreases radiation dose and less need for a contrast agent for CTCA to detect CAV early in the disease process [43]. The advantage of CTCA is that it is accessible in most centers, has a relatively low cost compared to MRI, and has high-resolution images. In addition, based on CTCA, 2010 ISHLT has decreased the stenosis of coronary to 50% rather previous 70% for early diagnosis of CAV [3]. The disadvantages are radiation exposure; contrast cannot be used with renal dysfunction and does not give any information on coronary microvasculature. CTCA is considered a gatekeeper for coronary angiography. An example of early detection of CAV in an 18-year-old HT recipient is shown in Figure 4. However, using CTCA in younger HT recipients has been challenging because of their high heart rate, small vessel size, and inability to lie still or hold their breath.

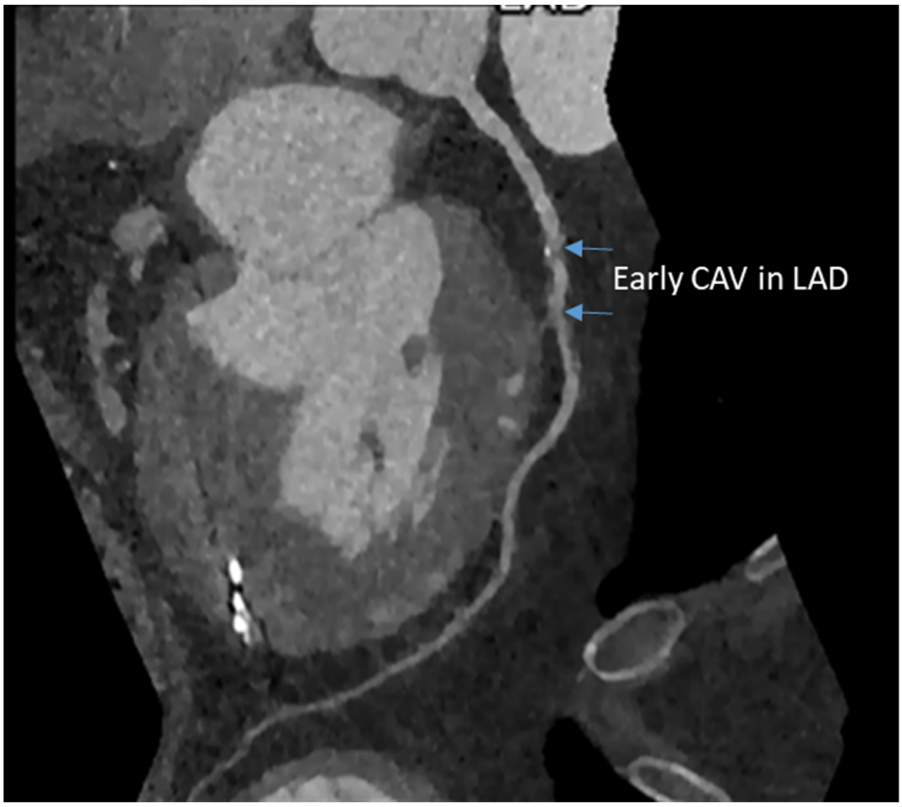


**Figure 4.** Early CAV in the left anterior descending coronary artery in an 18 yr old male six years after heart transplantation.

## 5. CMR Imaging

The CMR produces high-resolution images that allow accurate and reproducible cardiac chamber size and systolic function measurement. CMR can assess diastolic function, regional myocardial mechanics, and strain with a range of dedicated acquisitions and post-processing techniques. A significant strength of CMR with T2 and T1 mapping is in characterizing myocardial tissue properties: T1 mapping quantify myocyte damage and fibrosis, and T2 mapping help in determining myocardial edema. Using T2 mapping and extracellular volume (ECV) quantification in HT recipients provides high diagnostic accuracy for acute rejection. It could potentially decrease the number of routine EMBs [44]. In addition, native T1 time and ECV correlate with collagen volume in pediatric HT recipients [45]. In adults, CMR technology has been used since the 1980s and has shown helpful in detecting acute rejection and CAV [46–48]. Despite significant advancements related to CMR-based diagnosis of rejection and CAV in adults, there remain challenges in differentiating normal from abnormal in pediatric HT recipients because of the lack of pediatric normative data for quantitative parametric tissue mapping and variability in native T1 values depending upon the static magnetic field intensity (1.5 T vs. 3 T). Furthermore, age and gender might affect the T1 values, but there is currently no consensus about their effect.

CMR is superior to traditional visual analyses to detect regional wall motion abnormalities in children. In a study, Dedieu et al. showed that CMR effectively detected regional wall motion abnormalities corresponding to angiographic CAV in three patients that were not detected on echocardiography [49]. Tissue characterization by CMR allows quantification of ECV changes, which have been shown to correlate with diffuse myocardial fibrosis in 25 pediatric HT recipients aged 7.0 $\pm$ 6.3 years at transplant and 10.7 $\pm$ 6.5 years post-transplant and represent biological indicators of cardiac function after pediatric HT [50]. In another study by Hussain et al., 26 pediatric HT recipients underwent CTCA, IVUS, and stress CMR with tissue characterization, which showed that increasing T2 values were associated with worsening LV function and increasing T1/ECV and T2 values were associated with rejection burden and low-grade CAV [51]. However, LGE in adult HT recipients was not found to correlate with acute cellular rejection [52]. CMR imaging with quantitative T2 mapping offers a potential noninvasive method for screening pediatric HT patients for acute allograft rejection [53,54].

Conversely, a small CMR study using T2-weighted signal intensities and native T1 times, extracellular volumes, and LGE did not reliably identify acute cellular rejection in children [52]. However, the study was likely underpowered to detect the outcome. Automatic CMR-derived myocardial blood flow quantification is feasible in pediatric patients, and the technology could be potentially used for objective noninvasive assessment of CAV in children after HT [53–56]. Future studies are needed to establish the role of CMR parametric imaging using revised Lake Luis Consensus criteria [57] to identify acute rejection in pediatric HT recipients. The disadvantage is that younger patients need sedation or anesthesia to acquire CMR due to their inability to lie still or hold their breath. Furthermore, in the presence of stents or pacemakers, creating artifacts and images is challenging for interpretation.

*Adenosine Stress Perfusion Cardiac Magnetic Resonance Imaging*

Myocardial perfusion reserve measured by CMR is valuable and accurate in diagnosing adult CAV [57]. Myocardial perfusion reserve is the ratio of the myocardial blood flow during hyperemia to the myocardial blood flow at rest. Few studies showed that adenosine perfusion CMR imaging could be performed safely even in higher grade CAV in pediatric HT recipients [58]. Figure 5 illustrates an adenosine perfusion study in a 17-year-old HT recipient showing inferior ischemia and perfusion defect that correlates to CAV in the coronary angiogram.

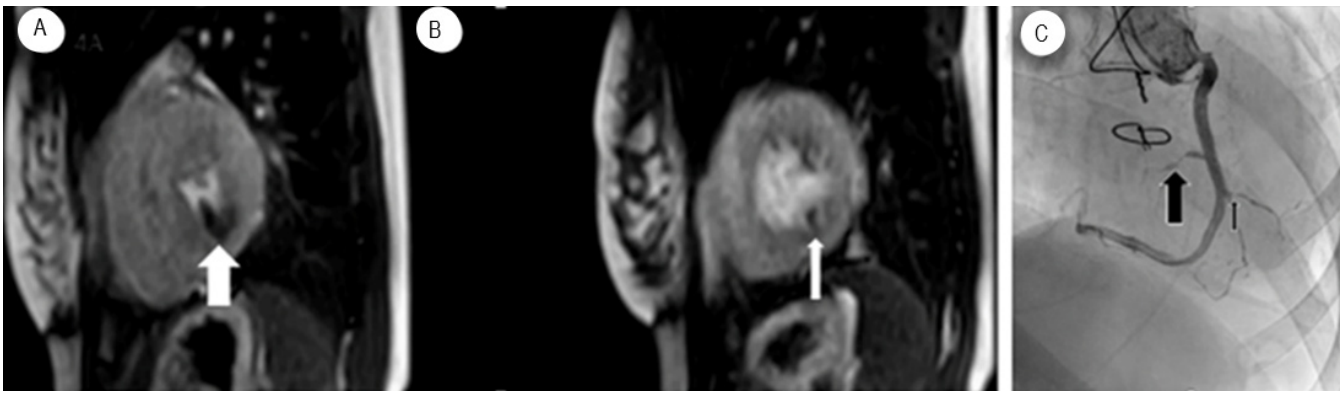


**Figure 5.** (**A**,**B**) MRI Perfusion images showing inferior ischemia induced by Adenosine (white arrow) in a patient with known CAV (**C**) Black arrows showing stenosis on selective coronary angiogram.

## 6. Intracoronary Imaging

Coronary angiography is the accepted clinical standard for CAV diagnosis (Figure 6A,B). However, there are pitfalls in current ISHL grading for CAV based on coronary angiography. The categorical grading from CAV0 to CAV3 is based on discrete rather than continuous metrics [3]. This classification only detects more significant changes such as >70%, which is the cutoff for single primary vessel stenosis to be grouped as CAV2. A diagnostic test is better if it has higher accuracy, more reproducibility, is less invasive, less costly, has better significance for prognosis, and is useful to guide treatment. Intracoronary imaging with IVUS and OCT is better for diagnosing early CAV and satisfies many criteria for better imaging modalities.

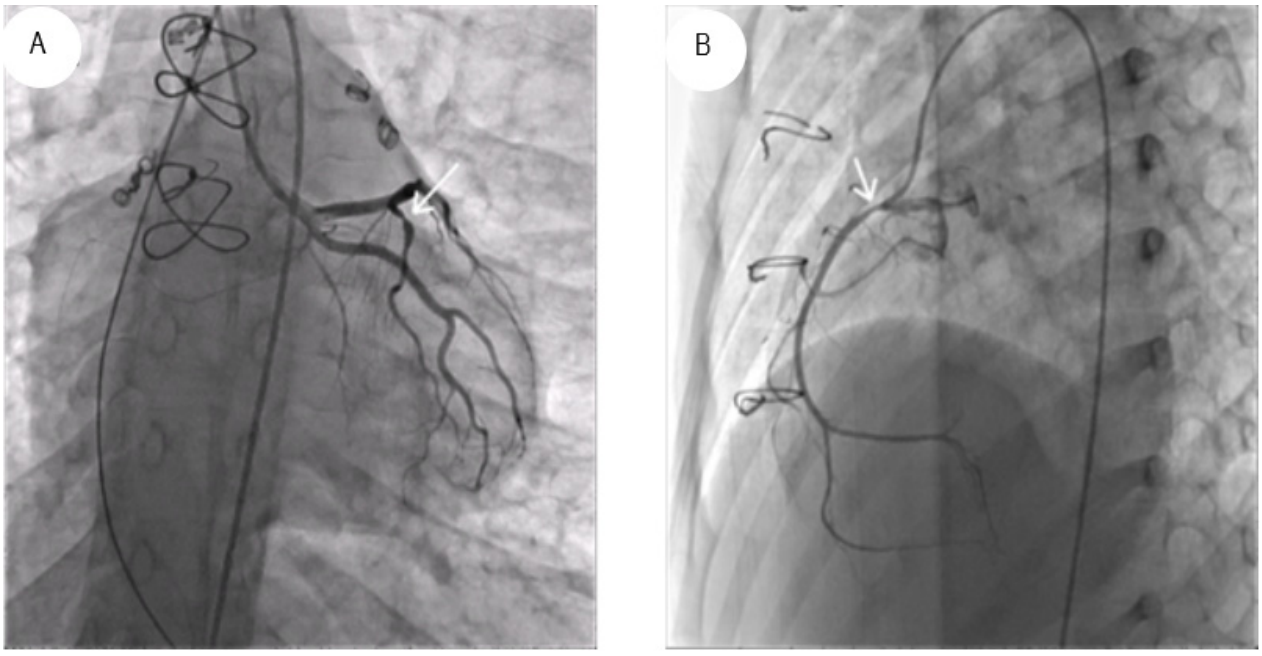


**Figure 6.** Show severe epicardial CAV in the left (**A**) and right coronary artery (**B**).

### *6.1. Intravascular Ultrasound*

IVUS has been increasingly utilized over the years as it allows for earlier and more accurate detection of early and progressive changes in the coronary vasculature. IVUS has been extensively studied in adults and has emerged as an excellent tool for a more precise quanti-

tative assessment of lumen size and intimal thickening [10]. In adults, the modified Stanford classification [59], based on intimal thickening, has been used for diagnosis and the severity of CAV: Class 1 (minimal) intimal thickness < 0.3 mm and extent of plaque < 180 degrees; Class 2 (mild) intimal thickness < 0.3 and extent of plaque > 180 degrees; Class 3 (moderate) intimal thickness 0.3–1 mm and plaque extent < 180 degrees; and Class 4 (severe) intimal thickness $\geq$ 1 mm and extent of plaque > 180 degrees. In adults, an intimal thickness of >0.5 mm by IVUS is associated with nonfatal major cardiac events and/or graft loss [60]. Furthermore, more recent data showed prognostic relevance of intimal thickness > 0.35 mm by IVUS within 1 and 5 years of HT [61]. However, IVUS is technically more challenging and is associated with increased procedural risk, including coronary artery spasms and a reported risk of coronary artery dissections in as many as 1.6% of catheterizations [62]. In pediatric HT recipients, IVUS has been limited by patient size and size of available catheters, and IVUS has not shown any correlation with microvascular disease [63]. However, a single-center pediatric study by Kuhn et al. described their experience using IVUS in 30 children seven years or older. The authors concluded that IVUS was more sensitive than angiography in detecting early CAV [64]. Figure 7 describes IVUS findings of early and progressive increase in intimal thickness in pediatric patients after HT. The limitations of IVUS are: optimum imaging protocol is not defined, it is limited to epicardial coronary arteries with sufficient lumen, and no large-scale randomized trial in children is carried out to demonstrate IVUS guided strategy improves outcomes.

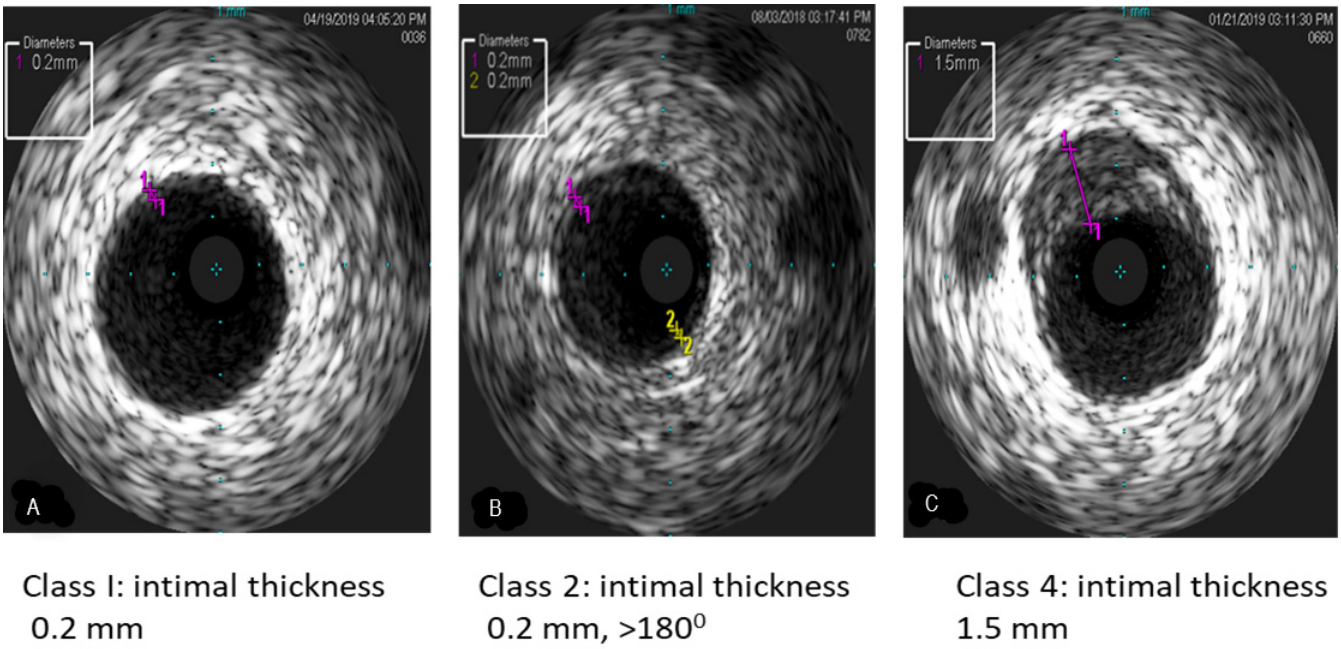


**Figure 7.** The illustration of IVUS shows the progression of CAV. (**A**) Class 1 (minimal) < 0.3 mm intimal thickening, (**B**) Class 2 (mild) < 0.3 mm intimal thickness and >180 degrees; and (**C**) Class 4 (severe) intimal thickness 1.5 mm.

### *6.2. Coronary Flow Reserve*

The concept of coronary flow reserve (CFR) is developed to describe the flow increase available to the heart in response to increased oxygen demand. CFR represents the vasodilator capacity of the coronary vascular bed during hyperemia and is measured by indicator thermodilution. CFR is expressed as the ratio between maximal hyperemic flow (after intracoronary adenosine injection) and resting flow. A descriptive vie of CFR is shown in Figure 8. In general, CFR > 2 is considered normal. In the presence of coronary stenosis, there is already vasodilation of the coronary artery distal to the stenosis, and there is diminished further dilation of coronary circulation after administration of adenosine,

and thus CFR is reduced [65]. A decrease in CFR after adenosine administration to achieve maximum vasodilation without significant epicardial stenosis indicates microvascular dysfunction. CFR data in children is limited. In a small study including 33 patients, 17 had epicardial coronary artery stenosis, CFR was reduced and correlated with histopathologic and angiographic evidence of microvascular disease [66]. CFR can also be measured by transthoracic Doppler echocardiography, and its feasibility and good correlation with myocardial perfusion study are shown in children with Kawasaki disease [67].

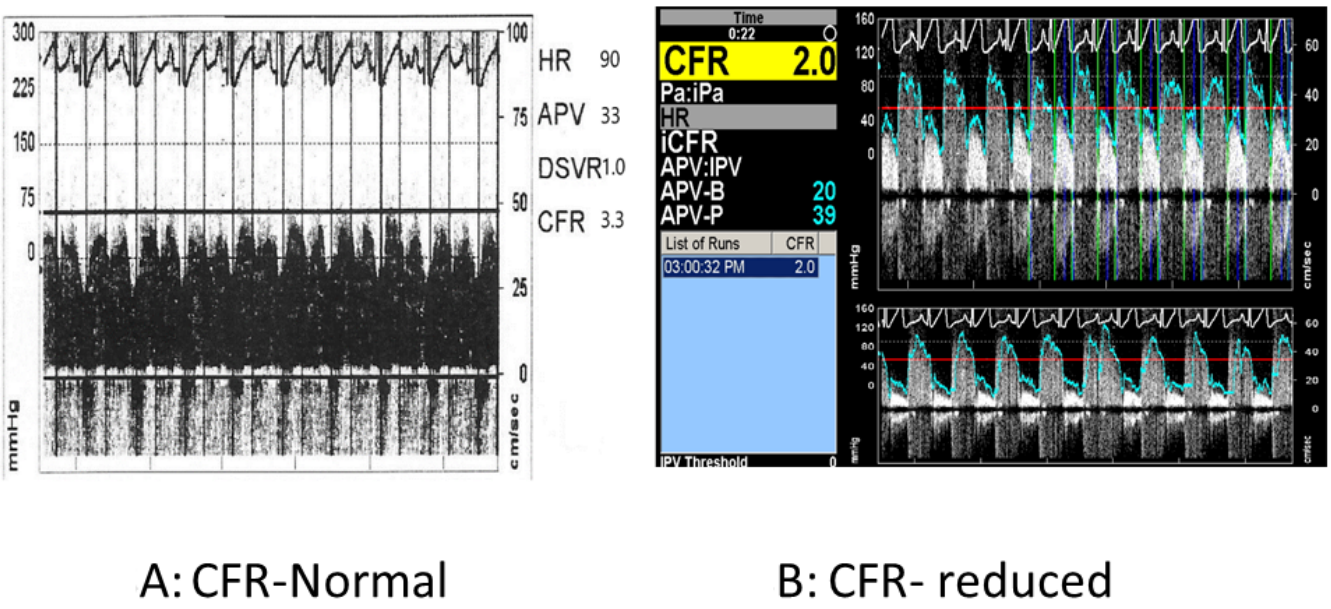


**Figure 8.** (**A**,**B**). Serial CFR at the time of cardiac catheterization and angiography in a pediatric HT recipient.

### *6.3. Optical Coherence Tomography*

OCT is an intracoronary imaging technique. The technique is similar to IVUS but relies on the signal derived from the backscatter of light from a near-infrared frequency beam [11]. Figure 9 demonstrates a cross-sectional and longitudinal view of the coronary vessel and intimal thickness. The reflection time to the light probe is measured, and the characteristics of structures are inferred. The short wavelength of light results in images with a better resolution than IVUS (10 to 20 nm vs. 100 to 150 nm) [68]. The different properties of tissue, and the subsequent effect on backscatter, mean that it is possible to develop "virtual histology" of the vessel wall. OCT resolution is higher and has a good correlation and interobserver variability than IVUS. However, specialized personnel and availability in most centers are needed. OCT can provide important insights into coronary vascular changes not detected by angiography on pediatric transplant patients and correlates well with the intimal thickness measured by IVUS [69]. Pediatric data is limited; however, a study in 73 children after HT (258 vessel segments) showed a high prevalence of segmental and eccentric intimal thickening [70]. However, another study in late survivors after pediatric HT reported that OCT findings of vulnerable plaque and complicated coronary lesions are rare, in contrast with adult HT recipients [71]. Further prospective and more extensive studies are needed to study the clinical utility of OCT to demonstrate its prognostic implications in children.

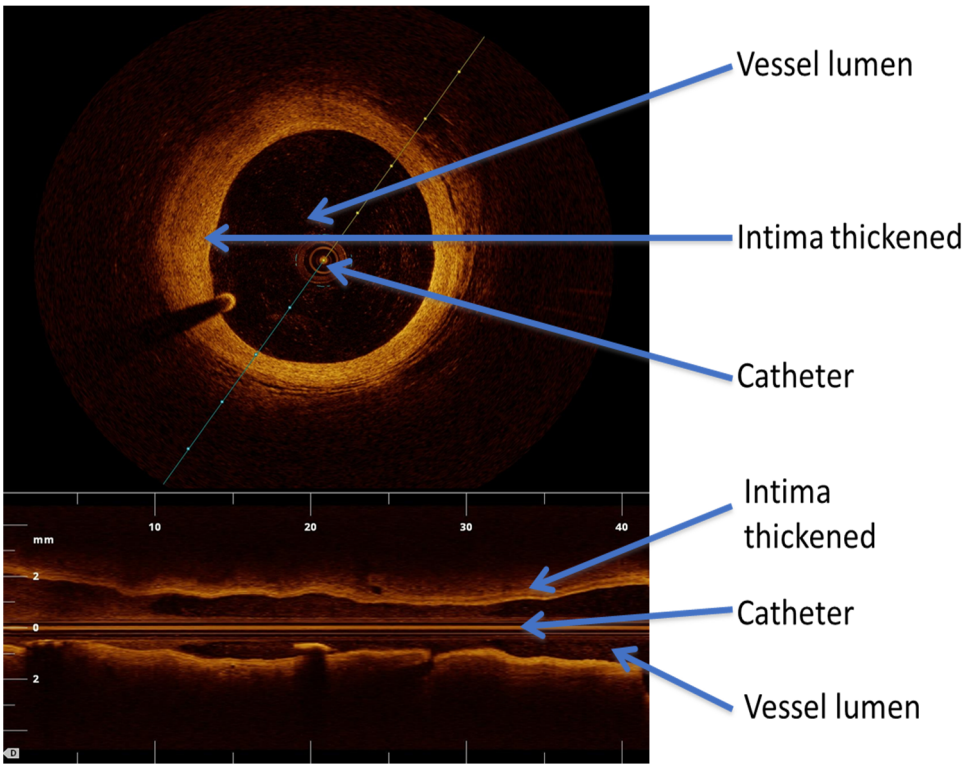


**Figure 9.** OCT images of a cross-sectional and longitudinal view of a coronary vessel. (This figure is adapted from reference: [72]. An open access journal).

## 7. Single-Photon Emission Computed Tomography

SPECT is a myocardial perfusion imaging technique to detect coronary blood flow to the myocardium and is commonly used in adults to diagnose atherosclerotic coronary artery disease [73]. Either exercise or pharmacological stress can be employed to obtain stress SPECT imaging which is compared with resting images after injecting radioactive tracers such as the technetium-99 m. SPECT relies on accurately measuring the radiotracer activity and correlate with the number of radiotracers transported by arterial blood to the myocardium. SPECT stress perfusion scan detects areas of decreased perfusion, and its sensitivity and specificity are 73% and 87%, respectively, to diagnose CAV compared to coronary angiography [74]. In one study among adult HT recipients, quantitative SPECT analysis as a method for CAV surveillance is found to have modest diagnostic accuracy and has overall modest prognostic utility for all causes of mortality during the entire follow-up since transplant [75]. In children with coronary artery lesions due to Kawasaki disease, Mostafa et al. used Tc-99m tetrofosmin SPECT to identify significant coronary stenosis and perfusion defect before surgery and the disappearance of these defects following surgery with a high degree of diagnostic accuracy with sensitivity (94%), specificity (100%), and accuracy (95%) [76]. In a small study of 20 pediatric patients, the Tc-99m tetrofosmin SPECT showed myocardial perfusion defect in 6 patients and correlated with CAV by angiography [77]. The limitations of SPECT include availability in all transplant centers and expert personnel needed for interpretation.

## 8. Positron Emission Tomography

Positron emission tomography (PET) myocardial perfusion imaging evaluates absolute myocardial blood flow in regional and global myocardium. Quantitative myocardial perfusion imaging with PET relies on accurately measuring radio-tracer activity. Myocardial uptake and retention of radioactive tracers based on blood flow, cellular integrity, and metabolism. The myocardial flow reserve is determined by the maximal hyperemic blood

flow ratio to resting blood flow. It has a higher spatial resolution than SPECT imaging and is widely adopted for coronary artery disease in adults for diagnosis and risk stratification [78]. FDG [18F] PET in murine model cardiac rejection has been used to monitor the evolution of rejection, and [N] NH3 imaging was used to monitor perfusion. Both techniques were highly reproducible and accurate [79]. PET is a noninvasive test, requires minimal radiation, no need for iodinated contrast, and has excellent diagnostic accuracy in moderate-severe CAV. The disadvantages of PET are its availability, significant expertise in interpretation needed, and limited external validation of PET in children.

## 9. Future Directions

The newer echocardiographic imaging is useful for quantitatively measuring myocardial function at the myocardial segment level. It provides better insight into graft dysfunction, sub-clinical rejection, response to rejection treatment, and early CAV. Coronary angiography is the gold standard for diagnosis of CAV, but intracoronary imaging techniques, including IVUS and OCT, can detect early CAV based on intimal thickness. CTCA and CMR techniques are noninvasive tests to detect CAV and are increasingly used in clinical practice in children. PET and SPECT imaging helps assess myocardial blood flow but is rarely used in children due to lack of standardization, availability, and need for expert personnel for interpretation.

## 10. Conclusions

In summary, HT involves a complex decision process and includes multi-disciplinary care to process various cardiac issues, including rejection and CAV. Multimodality imaging should be adopted to interrogate a failing graft when the etiology is unclear, with additional techniques used at each stage in the decision pathway individualized for the patient. It is also vital to align patient care with resource intensity such as cost, expert personnel, and availability of appropriately validated tests. There is a need for consistency and reliability in the interpretation of each test used for post-HT care, including EMB and imaging results. Artificial intelligence is a promising method where machine learning and creating algorithms may facilitate improvement in our ability to utilize multimodality imaging to prevent rejection and CAV in the future.

**Author Contributions:** B.B.D. Collected the data, drafted the manuscript and revised it, T.H. Contributed to revisions, critical review of this manuscript, and added figures to the paper, S.D. Contributed to data collection and critical review of this manuscript. All authors have read and agreed to the published version of the manuscript.

**Funding:** This research received no external funding.

**Institutional Review Board Statement:** Not applicable as this is a review paper.

**Informed Consent Statement:** Not applicable as this is a Review.

**Data Availability Statement:** The images are available with corresponding authors.

**Conflicts of Interest:** The authors declare no conflict of interest.

## References

1. Vanderlaan, R.D.; Manlhiot, C.; Edwards, L.B.; Conway, J.; McCrindle, B.W.; Dipchand, A.I. Risk factors for specific causes of death following pediatric heart transplant: An analysis of the registry of the International Society of Heart and Lung Transplantation. *Pediatr. Transpl.* **2015**, *19*, 896–905. [CrossRef] [PubMed]
2. Almond, C.S.; Hoen, H.; Rossano, J.W.; Castleberry, C.; Auerbach, S.R.; Yang, L.; Lal, A.K.; Everitt, M.D.; Fenton, M.; Hollander, S.A.; et al. Development and validation of a major adverse transplant event (MATE) score to predict late graft loss in pediatric heart transplantation. *J. Heart Lung Transpl.* **2018**, *37*, 441–450. [CrossRef] [PubMed]
3. Costanzo, M.R.; Dipchand, A.; Starling, R.; Anderson, A.; Chan, M.; Desai, S.; Fedson, S.; Fisher, P.; Gonzales-Stawinski, G.; Martinelli, L.; et al. The International Society of Heart and Lung Transplantation Guidelines for the care of heart transplant recipients. *J. Heart Lung Transpl.* **2010**, *29*, 914–956. [CrossRef] [PubMed]

4. Pophal, S.G.; Sigfusson, G.; Booth, K.L.; Bacanu, S.A.; Webber, S.A.; Ettedgui, J.A.; Neches, W.H.; Park, S.C. Complications of endomyocardial biopsy in children. *J. Am. Coll Cardiol.* **1999**, *34*, 2105–2110. [CrossRef]
5. Fyfe, D.A.; Ketchum, D.; Lewis, R.; Sabatier, J.; Kanter, K.; Mahle, W.; Vincent, R. Tissue Doppler imaging detects severely abnormal myocardial velocities that identify children with pre-terminal cardiac graft failure after heart transplantation. *J. Heart Lung Transpl.* **2006**, *25*, 510–517. [CrossRef]
6. Godown, J.; McEachern, W.A.; Dodd, D.A.; Stanley, M.; Havens, C.; Xu, M.; Slaughter, J.C.; Bearl, D.W.; Soslow, J.H. Temporal changes in left ventricular strain with the development of rejection in paediatric heart transplant recipients. *Cardiol. Young* **2019**, *29*, 954–959. [CrossRef]
7. Godown, J.; Cantor, R.; Koehl, D.; Cummings, E.; Vo, J.B.; Dodd, D.A.; Lytrivi, I.; Boyle, G.J.; Sutcliffe, D.L.; Kleinmahon, J.A.; et al. Practice variation in the diagnosis of acute rejection among pediatric heart transplant centers: An analysis of the pediatric heart transplant society (PHTS) registry. *J. Heart Lung Transpl.* **2021**, *40*, 1550–1559. [CrossRef]
8. Asante-Korang, A.; Fickey, M.; Boucek, M.M.; Boucek, R.J., Jr. Diastolic performance assessed by tissue Doppler after pediatric heart transplantation. *J. Heart Lung Transpl.* **2004**, *23*, 865–872. [CrossRef]
9. Giacomin, E.; Gasperini, S.; Zaca, V.; Ballo, P.; Diciolla, F.; Bernazzali, S.; Maccherini, M.; Galderisi, M.; Chiavarelli, M.; Mondillo, S. Relationship between coronary microcirculatory dysfunction and left ventricular long-axis function in heart transplant recipients. *J. Heart Lung Transpl.* **2007**, *26*, 1349–1350. [CrossRef]
10. Mondillo, S.; Maccherini, M.; Galderisi, M. Usefulness and limitations of transthoracic echocardiography in heart transplantation recipients. *Cardiovasc. Ultrasound* **2008**, *6*, 2. [CrossRef]
11. Badano, L.P.; Miglioranza, M.H.; Edvardsen, T.; Colafranceschi, A.S.; Muraru, D.; Bacal, F.; Nieman, K.; Zoppellaro, G.; Marcondes Braga, F.G.; Binder, T.; et al. European Association of Cardiovascular Imaging/Cardiovascular Imaging Department of the Brazilian Society of Cardiology recommendations for the use of cardiac imaging to assess and follow patients after heart transplantation. *Eur. Heart J. Cardiovasc. Imag.* **2015**, *16*, 919–948. [CrossRef] [PubMed]
12. Chowdhury, S.M.; Butts, R.J.; Hlavacek, A.M.; Taylor, C.L.; Chessa, K.S.; Bandisode, V.M.; Shirali, G.S.; Nutting, A.; Baker, G.H. Echocardiographic Detection of Increased Ventricular Diastolic Stiffness in Pediatric Heart Transplant Recipients: A Pilot Study. *J. Am. Soc. Echocardiogr.* **2018**, *31*, 342–348.e1. [CrossRef] [PubMed]
13. Eun, L.Y.; Gajarski, R.J.; Graziano, J.N.; Ensing, G.J. Relation of left ventricular diastolic function as measured by echocardiography and pulmonary capillary wedge pressure to rejection in young patients (< or = 31 years) after heart transplantation. *Am. J. Cardiol.* **2005**, *96*, 857–860. [CrossRef] [PubMed]
14. Pauliks, L.B.; Pietra, B.A.; DeGroff, C.G.; Kirby, K.S.; Knudson, O.A.; Logan, L.; Boucek, M.M.; Valdes-Cruz, L.M. Non-invasive detection of acute allograft rejection in children by tissue Doppler imaging: Myocardial velocities and myocardial acceleration during isovolumic contraction. *J. Heart Lung Transpl.* **2005**, *24*, S239–S248. [CrossRef] [PubMed]
15. Eidem, B.W.; McMahon, C.J.; Cohen, R.R.; Wu, J.; Finkelshteyn, I.; Kovalchin, J.P.; Ayres, N.A.; Bezold, L.I.; O'Brian Smith, E.; Pignatelli, R.H. Impact of cardiac growth on Doppler tissue imaging velocities: A study in healthy children. *J. Am. Soc. Echocardiogr.* **2004**, *17*, 212–221. [CrossRef]
16. Behera, S.K.; Trang, J.; Feeley, B.T.; Levi, D.S.; Alejos, J.C.; Drant, S. The use of Doppler tissue imaging to predict cellular and antibody-mediated rejection in pediatric heart transplant recipients. *Pediatr. Transpl.* **2008**, *12*, 207–214. [CrossRef]
17. Goldberg, D.J.; Quartermain, M.D.; Glatz, A.C.; Hall, E.K.; Davis, E.; Kren, S.A.; Hanna, B.D.; Cohen, M.S. Doppler tissue imaging in children following cardiac transplantation: A comparison to catheter derived hemodynamics. *Pediatr. Transpl.* **2011**, *15*, 488–494. [CrossRef] [PubMed]
18. Sachdeva, R.; Malik, S.; Seib, P.M.; Frazier, E.A.; Cleves, M.A. Doppler tissue imaging and catheter-derived measures are not independent predictors of rejection in pediatric heart transplant recipients. *Int. J. Cardiovasc. Imag.* **2011**, *27*, 947–954. [CrossRef]
19. Lunze, F.I.; Singh, T.P.; Gauvreau, K.; Molloy, M.A.; Blume, E.D.; Berger, F.; Colan, S.D. Comparison of tissue Doppler imaging and conventional echocardiography to discriminate rejection from non-rejection after pediatric heart transplantation. *Pediatr. Transpl.* **2020**, *24*, e13738. [CrossRef]
20. Hernandez, L.E.; Shepard, C.W.; Menk, J.; Lilliam, V.C.; Ameduri, R.K. Global left ventricular relaxation: A novel tissue Doppler index of acute rejection in pediatric heart transplantation. *J. Heart Lung Transpl.* **2015**, *34*, 1190–1197. [CrossRef]
21. Hernandez, L.E.; Chrisant, M.K.; Valdes-Cruz, L.M. Global Left Ventricular Relaxation: A Useful Echocardiographic Marker of Heart Transplant Rejection and Recovery in Children. *J. Am. Soc. Echocardiogr.* **2019**, *32*, 529–536. [CrossRef] [PubMed]
22. Patel, M.D.; Myers, C.; Negishi, K.; Singh, G.K.; Anwar, S. Two-Dimensional Strain is more Precise than Conventional Measures of Left Ventricular Systolic Function in Pediatric Patients. *Pediatr. Cardiol.* **2020**, *41*, 186–193. [CrossRef] [PubMed]
23. Chowdhury, S.M.; Butts, R.J.; Taylor, C.L.; Bandisode, V.M.; Chessa, K.S.; Hlavacek, A.M.; Nutting, A.; Shirali, G.S.; Baker, G.H. Longitudinal measures of deformation are associated with a composite measure of contractility derived from pressure-volume loop analysis in children. *Eur. Heart J. Cardiovasc. Imag.* **2018**, *19*, 562–568. [CrossRef]
24. Goudar, S.P.; Baker, G.H.; Chowdhury, S.M.; Reid, K.J.; Shirali, G.; Scheurer, M.A. Interpreting measurements of cardiac function using vendor-independent speckle tracking echocardiography in children: A prospective, blinded comparison with catheter-derived measurements. *Echocardiography* **2016**, *33*, 1903–1910. [CrossRef]
25. Parthiban, A.; Jani, V.; Zhang, J.; Li, L.; Craft, M.; Barnes, A.; Ballweg, J.A.; Schuster, A.; Danford, D.A.; Kutty, S. Altered Biatrial Phasic Function after Heart Transplantation in Children. *J. Am. Soc. Echocardiogr.* **2020**, *33*, 1132–1140.e1132. [CrossRef]

26. Engelhardt, K.; Das, B.; Sorensen, M.; Malik, S.; Zellers, T.; Lemler, M. Two-dimensional systolic speckle tracking echocardiography provides a noninvasive aid in the identification of acute pediatric heart transplant rejection. *Echocardiography* **2019**, *36*, 1876–1883. [CrossRef] [PubMed]
27. Boucek, K.; Burnette, A.; Henderson, H.; Savage, A.; Chowdhury, S.M. Changes in circumferential strain can differentiate pediatric heart transplant recipients with and without graft rejection. *Pediatr. Transpl.* **2022**, *26*, e14195. [CrossRef] [PubMed]
28. Wisotzkey, B.L.; Jorgensen, N.W.; Albers, E.L.; Kemna, M.S.; Boucek, R.J.; Kronmal, R.A.; Law, Y.M.; Bhat, A.H. Feasibility and interpretation of global longitudinal strain imaging in pediatric heart transplant recipients. *Pediatr. Transpl.* **2017**, *21*, 12909. [CrossRef]
29. Antonczyk, K.; Niklewski, T.; Antonczyk, R.; Zakliczynski, M.; Zembala, M.; Kukulski, T. Speckle-Tracking Echocardiography for Monitoring Acute Rejection in Transplanted Heart. *Transpl. Proc.* **2018**, *50*, 2090–2094. [CrossRef]
30. Gursu, H.A.; Varan, B.; Sade, E.; Erdogan, I.; Sezgin, A.; Aslamaci, S. Evaluation of Acute Rejection by Measuring Strain and Strain Rate in Children With Heart Transplant: A Preliminary Report. *Exp. Clin. Transpl.* **2017**, *15*, 561–566. [CrossRef]
31. Buddhe, S.; Richmond, M.E.; Gilbreth, J.; Lai, W.W. Longitudinal Strain by Speckle Tracking Echocardiography in Pediatric Heart Transplant Recipients. *Congenit. Heart Dis.* **2015**, *10*, 362–370. [CrossRef] [PubMed]
32. Yeh, J.; Aiyagari, R.; Gajarski, R.J.; Zamberlan, M.C.; Lu, J.C. Left atrial deformation predicts pulmonary capillary wedge pressure in pediatric heart transplant recipients. *Echocardiography* **2015**, *32*, 535–540. [CrossRef] [PubMed]
33. Boruta, R.J.; Miyamoto, S.D.; Younoszai, A.K.; Patel, S.S.; Landeck, B.F., 2nd. Worsening in Longitudinal Strain and Strain Rate Anticipates Development of Pediatric Transplant Coronary Artery Vasculopathy as Soon as One Year Following Transplant. *Pediatr. Cardiol.* **2018**, *39*, 129–139. [CrossRef] [PubMed]
34. Yeung, J.P.; Human, D.G.; Sandor, G.G.; De Souza, A.M.; Potts, J.E. Serial measurements of exercise performance in pediatric heart transplant patients using stress echocardiography. *Pediatr. Transpl.* **2011**, *15*, 265–271. [CrossRef] [PubMed]
35. Pahl, E.; Crawford, S.E.; Swenson, J.M.; Duffy, C.E.; Fricker, F.J.; Backer, C.L.; Mavroudis, C.; Chaudhry, F.A. Dobutamine stress echocardiography: Experience in pediatric heart transplant recipients. *J. Heart Lung Transpl.* **1999**, *18*, 725–732. [CrossRef]
36. Dipchand, A.I.; Bharat, W.; Manlhiot, C.; Safi, M.; Lobach, N.E.; McCrindle, B.W. A prospective study of dobutamine stress echocardiography for the assessment of cardiac allograft vasculopathy in pediatric heart transplant recipients. *Pediatr. Transpl.* **2008**, *12*, 570–576. [CrossRef]
37. Fine, N.M.; Greenway, S.C.; Mulvagh, S.L.; Huang, R.Q.; Maxon, S.A.; Hepinstall, M.J.; Anderson, J.H.; Johnson, J.N. Feasibility of Real-Time Myocardial Contrast Echocardiography to Detect Cardiac Allograft Vasculopathy in Pediatric Heart Transplant Recipients. *J. Am. Soc. Echocardiog.* **2021**, *34*, 503–510. [CrossRef]
38. Larsen, R.L.; Applegate, P.M.; Dyar, D.A.; Ribeiro, P.A.; Fritzsche, S.D.; Mulla, N.F.; Shirali, G.S.; Kuhn, M.A.; Chinnock, R.E.; Shah, P.M. Dobutamine stress echocardiography for assessing coronary artery disease after transplantation in children. *J. Am. Coll Cardiol.* **1998**, *32*, 515–520. [CrossRef]
39. Di Filippo, S.; Semiond, B.; Roriz, R.; Sassolas, F.; Raboisson, M.J.; Bozio, A. Non-invasive detection of coronary artery disease by dobutamine-stress echocardiography in children after heart transplantation. *J. Heart Lung Transpl.* **2003**, *22*, 876–882. [CrossRef]
40. Cifra, B.; Morgan, C.T.; Dragulescu, A.; Guerra, V.C.; Slorach, C.; Friedberg, M.K.; Manlhiot, C.; McCrindle, B.W.; Dipchand, A.I.; Mertens, L. Right ventricular function during exercise in children after heart transplantation. *Eur. Heart J. Cardiovasc. Imag.* **2018**, *19*, 647–653. [CrossRef]
41. Clemmensen, T.S.; Eiskjaer, H.; Logstrup, B.B.; Tolbod, L.P.; Harms, H.J.; Bouchelouche, K.; Hoff, C.; Frokiaer, J.; Poulsen, S.H. Noninvasive Detection of Cardiac Allograft Vasculopathy by Stress Exercise Echocardiographic Assessment of Myocardial Deformation. *J. Am. Soc. Echocardiogr.* **2016**, *29*, 480–490. [CrossRef] [PubMed]
42. Nous, F.M.A.; Roest, S.; van Dijkman, E.D.; Attrach, M.; Caliskan, K.; Brugts, J.J.; Nieman, K.; Hirsch, A.; Constantinescu, A.A.; Manintveld, O.C.; et al. Clinical implementation of coronary computed tomography angiography for routine detection of cardiac allograft vasculopathy in heart transplant patients. *Transpl. Int.* **2021**, *34*, 1886–1894. [CrossRef] [PubMed]
43. Si-Mohamed, S.A.; Boccalini, S.; Lacombe, H.; Diaw, A.; Varasteh, M.; Rodesch, P.A.; Dessouky, R.; Villien, M.; Tatard-Leitman, V.; Bochaton, T.; et al. Coronary CT Angiography with Photon-counting CT: First-In-Human Results. *Radiology* **2022**, *303*, 303–313. [CrossRef]
44. Vermes, E.; Pantaleon, C.; Auvet, A.; Cazeneuve, N.; Machet, M.C.; Delhommais, A.; Bourguignon, T.; Aupart, M.; Brunereau, L. Cardiovascular magnetic resonance in heart transplant patients: Diagnostic value of quantitative tissue markers: T2 mapping and extracellular volume fraction, for acute rejection diagnosis. *J. Cardiovasc. Magn. Reson.* **2018**, *20*, 59. [CrossRef]
45. Ide, S.; Riesenkampff, E.; Chiasson, D.A.; Dipchand, A.I.; Kantor, P.F.; Chaturvedi, R.R.; Yoo, S.J.; Grosse-Wortmann, L. Histological validation of cardiovascular magnetic resonance T1 mapping markers of myocardial fibrosis in paediatric heart transplant recipients. *J. Cardiovasc. Magn. Reson.* **2017**, *19*, 10. [CrossRef] [PubMed]
46. Aherne, T.; Tscholakoff, D.; Finkbeiner, W.; Sechtem, U.; Derugin, N.; Yee, E.; Higgins, C.B. Magnetic resonance imaging of cardiac transplants: The evaluation of rejection of cardiac allografts with and without immunosuppression. *Circulation* **1986**, *74*, 145–156. [CrossRef]
47. Sasaki, H.; Sada, M.; Nishimura, T.; Yutani, C.; Nakatani, H.; Yaku, H.; Yamaguchi, T.; Kawazoe, K.; Amemiya, H.; Fujita, T. The expanded scope of effectiveness of nuclear magnetic resonance imaging to determine cardiac allograft rejection. *Transpl. Proc.* **1987**, *19*, 1062–1064.

48. Wisenberg, G.; Pflugfelder, P.W.; Kostuk, W.J.; McKenzie, F.N.; Prato, F.S. Diagnostic applicability of magnetic resonance imaging in assessing human cardiac allograft rejection. *Am. J. Cardiol.* **1987**, *60*, 130–136. [CrossRef]
49. Dedieu, N.; Silva Vieira, M.; Fenton, M.; Wong, J.; Botnar, R.; Burch, M.; Greil, G.; Hussain, T. The importance of qualitative and quantitative regional wall motion abnormality assessment at rest in pediatric coronary allograft vasculopathy. *Pediatr. Transpl.* **2018**, *22*, e13208. [CrossRef]
50. Feingold, B.; Salgado, C.M.; Reyes-Mugica, M.; Drant, S.E.; Miller, S.A.; Kennedy, M.; Kellman, P.; Schelbert, E.B.; Wong, T.C. Diffuse myocardial fibrosis among healthy pediatric heart transplant recipients: Correlation of histology, cardiovascular magnetic resonance, and clinical phenotype. *Pediatr. Transpl.* **2017**, *21*, 12986. [CrossRef]
51. Husain, N.; Watanabe, K.; Berhane, H.; Gupta, A.; Markl, M.; Rigsby, C.K.; Robinson, J.D. Multi-parametric cardiovascular magnetic resonance with regadenoson stress perfusion is safe following pediatric heart transplantation and identifies history of rejection and cardiac allograft vasculopathy. *J. Cardiovasc. Magn. Reson.* **2021**, *23*, 135. [CrossRef] [PubMed]
52. Simsek, E.; Nalbantgil, S.; Ceylan, N.; Zoghi, M.; Kemal, H.S.; Engin, C.; Yagdi, T.; Ozbaran, M. Diagnostic performance of late gadolinium enhancement in the assessment of acute cellular rejection after heart transplantation. *Anatol. J. Cardiol.* **2016**, *16*, 113–118. [CrossRef] [PubMed]
53. Dolan, R.S.; Rahsepar, A.A.; Blaisdell, J.; Suwa, K.; Ghafourian, K.; Wilcox, J.E.; Khan, S.S.; Vorovich, E.E.; Rich, J.D.; Anderson, A.S.; et al. Multiparametric Cardiac Magnetic Resonance Imaging Can Detect Acute Cardiac Allograft Rejection After Heart Transplantation. *JACC Cardiovasc. Imag.* **2019**, *12*, 1632–1641. [CrossRef] [PubMed]
54. Sethi, N.; Doshi, A.; Doshi, T.; Cross, R.; Cronin, I.; Amin, E.; Kanter, J.; Scheel, J.; Khan, S.; Campbell-Washburn, A.; et al. Quantitative cardiac magnetic resonance T2 imaging offers ability to non-invasively predict acute allograft rejection in children. *Cardiol. Young* **2020**, *30*, 852–859. [CrossRef]
55. Greenway, S.C.; Dallaire, F.; Kantor, P.F.; Dipchand, A.I.; Chaturvedi, R.R.; Warade, M.; Riesenkampff, E.; Yoo, S.J.; Grosse-Wortmann, L. Magnetic resonance imaging of the transplanted pediatric heart as a potential predictor of rejection. *World J. Transpl.* **2016**, *6*, 751–758. [CrossRef]
56. Scannell, C.M.; Hasaneen, H.; Greil, G.; Hussain, T.; Razavi, R.; Lee, J.; Pushparajah, K.; Duong, P.; Chiribiri, A. Automated Quantitative Stress Perfusion Cardiac Magnetic Resonance in Pediatric Patients. *Front. Pediatr.* **2021**, *9*, 699497. [CrossRef]
57. Miller, C.A.; Sarma, J.; Naish, J.H.; Yonan, N.; Williams, S.G.; Shaw, S.M.; Clark, D.; Pearce, K.; Stout, M.; Potluri, R.; et al. Multiparametric cardiovascular magnetic resonance assessment of cardiac allograft vasculopathy. *J. Am. Coll Cardiol.* **2014**, *63*, 799–808. [CrossRef]
58. Duran, S.R.; Huffaker, T.; Dixon, B.; Gooty, V.; Abou Zahr, R.; Arar, Y.; Greer, J.S.; Butts, R.J.; Hussain, M.T. Feasibility and safety of quantitative adenosine stress perfusion cardiac magnetic resonance imaging in pediatric heart transplant patients with and without coronary allograft vasculopathy. *Pediatr. Radiol.* **2021**, *51*, 1311–1321. [CrossRef]
59. Rickenbacher, P.R.; Pinto, F.J.; Chenzbraun, A.; Botas, J.; Lewis, N.P.; Alderman, E.L.; Valantine, H.A.; Hunt, S.A.; Schroeder, J.S.; Popp, R.L.; et al. Incidence and severity of transplant coronary artery disease early and up to 15 years after transplantation as detected by intravascular ultrasound. *J. Am. Coll Cardiol.* **1995**, *25*, 171–177. [CrossRef]
60. Kobashigawa, J.A.; Tobis, J.M.; Starling, R.C.; Tuzcu, E.M.; Smith, A.L.; Valantine, H.A.; Yeung, A.C.; Mehra, M.R.; Anzai, H.; Oeser, B.T.; et al. Multicenter intravascular ultrasound validation study among heart transplant recipients: Outcomes after five years. *J. Am. Coll Cardiol.* **2005**, *45*, 1532–1537. [CrossRef] [PubMed]
61. Potena, L.; Masetti, M.; Sabatino, M.; Bacchi-Reggiani, M.L.; Pece, V.; Prestinenzi, P.; Dall'Ara, G.; Taglieri, N.; Saia, F.; Fallani, F.; et al. Interplay of coronary angiography and intravascular ultrasound in predicting long-term outcomes after heart transplantation. *J. Heart Lung Transpl.* **2015**, *34*, 1146–1153. [CrossRef] [PubMed]
62. Kindel, S.J.; Pahl, E. Current therapies for cardiac allograft vasculopathy in children. *Congenit. Heart Dis.* **2012**, *7*, 324–335. [CrossRef]
63. Nicolas, R.T.; Kort, H.W.; Balzer, D.T.; Trinkaus, K.; Dent, C.L.; Hirsch, R.; Canter, C.E. Surveillance for transplant coronary artery disease in infant, child and adolescent heart transplant recipients: An intravascular ultrasound study. *J. Heart Lung Transpl.* **2006**, *25*, 921–927. [CrossRef] [PubMed]
64. Kuhn, M.A.; Jutzy, K.R.; Deming, D.D.; Cephus, C.E.; Chinnock, R.E.; Johnston, J.; Bailey, L.L.; Larsen, R.L. The medium-term findings in coronary arteries by intravascular ultrasound in infants and children after heart transplantation. *J. Am. Coll Cardiol.* **2000**, *36*, 250–254. [CrossRef]
65. Spaan, J.A.; Piek, J.J.; Hoffman, J.I.; Siebes, M. Physiological basis of clinically used coronary hemodynamic indices. *Circulation* **2006**, *113*, 446–455. [CrossRef] [PubMed]
66. Schubert, S.; Abdul-Khaliq, H.; Wellnhofer, E.; Hiemann, N.E.; Ewert, P.; Lehmkuhl, H.B.; Meyer, R.; Miera, O.; Peters, B.; Hetzer, R.; et al. Coronary flow reserve measurement detects transplant coronary artery disease in pediatric heart transplant patients. *J. Heart Lung Transpl.* **2008**, *27*, 514–521. [CrossRef]
67. Hiraishi, S.; Hirota, H.; Horiguchi, Y.; Takeda, N.; Fujino, N.; Ogawa, N.; Nakahata, Y. Transthoracic Doppler assessment of coronary flow velocity reserve in children with Kawasaki disease: Comparison with coronary angiography and thallium-201 imaging. *J. Am. Coll Cardiol.* **2002**, *40*, 1816–1824. [CrossRef]
68. Pinto, T.L.; Waksman, R. Clinical applications of optical coherence tomography. *J. Interv. Cardiol.* **2006**, *19*, 566–573. [CrossRef]

69. McGovern, E.; Hosking, M.C.K.; Balbacid, E.; Voss, C.; Berger, F.; Schubert, S.; Harris, K.C. Optical Coherence Tomography for the Early Detection of Coronary Vascular Changes in Children and Adolescents After Cardiac Transplantation: Findings From the International Pediatric OCT Registry. *JACC Cardiovasc. Imag.* **2019**, *12*, 2492–2501. [CrossRef]
70. Lague, S.L.; Bone, J.N.; Samuel, R.; Voss, C.; Balbacid, E.; Hosking, M.C.K.; Schubert, S.; Harris, K.C. Patterns of Early Coronary Artery Changes in Pediatric Heart Transplant Recipients Detected Using Optical Coherence Tomography. *Circ Cardiovasc. Imag.* **2022**, *15*, e012486. [CrossRef]
71. Tomai, F.; De Luca, L.; Petrolini, A.; Di Vito, L.; Ghini, A.S.; Corvo, P.; De Persio, G.; Parisi, F.; Pongiglione, G.; Giulia Gagliardi, M.; et al. Optical coherence tomography for characterization of cardiac allograft vasculopathy in late survivors of pediatric heart transplantation. *J. Heart Lung Transpl.* **2016**, *35*, 74–79. [CrossRef] [PubMed]
72. Dedieu, N.; Greil, G.; Wong, J.; Fenton, M.; Burch, M.; Hussain, T. Diagnosis and management of coronary allograft vasculopaathy in children and adolescents. *World J. Transpl.* **2014**, *4*, 276–293. [CrossRef] [PubMed]
73. Shaw, L.J.; Berman, D.S.; Maron, D.J.; Mancini, G.B.; Hayes, S.W.; Hartigan, P.M.; Weintraub, W.S.; O'Rourke, R.A.; Dada, M.; Spertus, J.A.; et al. Optimal medical therapy with or without percutaneous coronary intervention to reduce ischemic burden: Results from the Clinical Outcomes Utilizing Revascularization and Aggressive Drug Evaluation (COURAGE) trial nuclear substudy. *Circulation* **2008**, *117*, 1283–1291. [CrossRef]
74. Klocke, F.J.; Baird, M.G.; Lorell, B.H.; Bateman, T.M.; Messer, J.V.; Berman, D.S.; O'Gara, P.T.; Carabello, B.A.; Russell, R.O., Jr.; Cerqueira, M.D.; et al. ACC/AHA/ASNC guidelines for the clinical use of cardiac radionuclide imaging–executive summary: A report of the American College of Cardiology/American Heart Association Task Force on Practice Guidelines (ACC/AHA/ASNC Committee to Revise the 1995 Guidelines for the Clinical Use of Cardiac Radionuclide Imaging). *Circulation* **2003**, *108*, 1404–1418. [CrossRef] [PubMed]
75. Aguilar, J.; Miller, R.J.H.; Otaki, Y.; Tamarappoo, B.; Hayes, S.; Friedman, J.; Slomka, P.J.; Thomson, L.E.J.; Kittleson, M.; Patel, J.K.; et al. Clinical Utility of SPECT in the Heart Transplant Population: Analysis From a Single Large-volume Center. *Transplantation* **2022**, *106*, 623–632. [CrossRef] [PubMed]
76. Mostafa, M.S.; Sayed, A.O.; Al Said, Y.M. Assessment of coronary ischaemia by myocardial perfusion dipyridamole stress technetium-99 m tetrofosmin, single-photon emission computed tomography, and coronary angiography in children with Kawasaki disease: Pre- and post-coronary bypass grafting. *Cardiol. Young* **2015**, *25*, 927–934. [CrossRef]
77. Maiers, J.; Hurwitz, R. Identification of coronary artery disease in the pediatric cardiac transplant patient. *Pediatr. Cardiol.* **2008**, *29*, 19–23. [CrossRef]
78. Singh, T.P.; Muzik, O.; Forbes, T.F.; Di Carli, M.F. Positron emission tomography myocardial perfusion imaging in children with suspected coronary abnormalities. *Pediatr. Cardiol.* **2003**, *24*, 138–144. [CrossRef]
79. Daly, K.P.; Dearling, J.L.; Seto, T.; Dunning, P.; Fahey, F.; Packard, A.B.; Briscoe, D.M. Use of [18F]FDG Positron Emission Tomography to Monitor the Development of Cardiac Allograft Rejection. *Transplantation* **2015**, *99*, e132–e139. [CrossRef]